Journal of KSNVE, Vol. 8, No. 6, pp. 1172~1180, 1998.

〈Original Paper〉

Numerical Analysis and Characteristics of Acoustic and Elastic Wave Scattering from Rigid or Soft Objects

강성 또는 연성 물체로 인한 음향파와 탄성파 산란의 수치해석 및 특성 분석

Huinam Rhee*
이 희 남

(Received July 25, 1998 : Accepted October 12, 1998)

Key Words : Acoustic Wave(음향파), Elastic Wave(탄성파), Scattering(산란), Scattered Wave(산란파), Partial Wave(부분파), Rigid Object(강성물체), Soft Object(연성물체), Phase(위상), Mode Conversion(모드변환), Longitudinal Wave(종파), Shear Wave (횡파)

ABSTRACT

Elastic wave scattering from an acoustically rigid or soft object is studied and compared with the acoustic wave scattering. The behavior of phases as well as magnitudes of partial waves and their total summation of scattered wave are numerically analyzed and discussed. The effect of mode conversion, which occurs between longitudinal and transversal waves in elastic wave scattering, on the magnitudes and phases of scattered waves is identified.

요 약

음향학적으로 강성인 물체와 연성인 물체로부터의 탄성파의 산란과 음향파의 산란을 수치적으로 해석하고 그 특성들을 비교하였다. 부분파들과, 또한 부분파들의 합인 전체 산란파의 위상 및 크기의 거동을 수치적으로 분석하고 토의 하였다. 탄성파의 산란시 발생하는 종파와 횡파 사이의 모드변환 현상이 산란파의 크기와 위상에 주는 영향을 밝혔다.

1. Introduction

The scattering of acoustic or elastic wave is a phenomenon which can easily be observed in nature. The problem of wave scattering has become a classical subject since the pioneer study by Lord Rayleigh[1] and its theoretical basis has been well-established by numerous authors such as Morse and Ingard[2], Bowman, *et al.* [3], etc. The scattering of waves is involved with complicated physical phenomena such as reflection, diffraction and refraction. If the object (scatterer) is acoustically impenetrable, the energy of the incident wave can not penerate into the object and consequently the scattering mechanism becomes relatively simple. We have two extreme cases for the impenetrable objects : one is rigid case of which acoustic impedance is infinite, and the other one is soft

* 정회원, 한국전력기술주식회사 원자로설계개발단

case of which acoustic impedance is zero. This paper deals with the scattering of acoustic or elastic wave from a rigid or soft infinitely-long cylindrical object. Although the wave scattering from impenetrable objects can be regarded as a classical problem, the magnitude of the scattered waves has usually been studied, while the study on the phase behavior has not been well established.

The importance of the phase of the scattered waves has recently been issued by Rhee and Park[4] for the case of resonance scattering[5~7] of acoustic waves, which is related with the eigenvibration of the elastic penetrable objects excited by the standing wave formed inside the objects. For a penetrable object, the vibrational resonance information of the scatterer is mixed with the acoustic background in the scattered wave. In many cases the acoustic background can be approximated as the scattering from impenetrable objects. According to Rhee and Park[4], it is important to understand the exact behavior (for both phase and magnitude) of the acoustic background for the isolation of vibrational resonance information of the elastic penetrable objects.

In this paper, we study the behavior of phase as well as magnitude of the scattered wave for acoustic and elastic wave scattering from impenetrable objects. Especially, the effect of mode conversion, which occurs between longitudinal and shear waves in elastic wave scattering, on the magnitude and phase of partial waves of scattered wave is to be discussed.

2. Acoustic Wave Scattering

Let us consider an infinite plane acoustic wave $p_0 \exp i(kX-\omega t)$ with a propagation constant $k=\omega/c$, where c is the speed of sound in the fluid medium, incident along the X - axis on a rigid or soft cylinder of radius a whose axis is coincides with the Z axis (Fig. 1). The acoustic impedance of the rigid (soft) cylinder is infinite

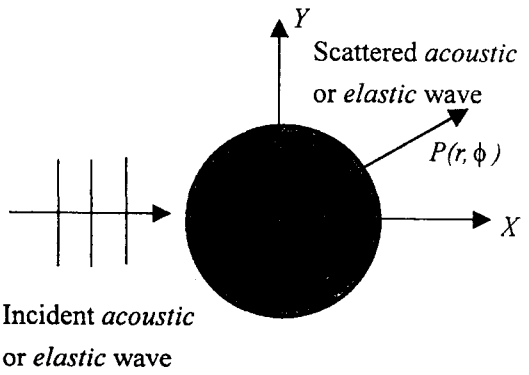

Fig. 1 Schematic of wave scattering from a cylindrical object

(zero) so that the incident wave can not penetrate into the cylinder at all. At a point $P(r,\phi)$ located in the fluid surrounding the cylinder, it produces the following scattered field P_{sc} :

$$P_{sc}(r,\phi)=p_0\sum_{n=0}^{\infty}\varepsilon_n i^n A_n(x)H_n^{(1)}(kr)\cos n\phi, \tag{1}$$

where the argument x of the cylindrical functions is a nondimensionalized frequency defined as $x=ka=\omega a/c$.

By applying a set of appropriate boundary conditions, i.e., continuities of stresses and displacements on the boundary surface of the cylinder, the unknown scattering coefficient A_n is determined as follows[5] :

For a rigid cylinder,

$$A_n(x)=A_n(x)^r=-\frac{J_n'(x)}{H_n^{(1)'}(x)} \tag{2}$$

For a soft cylinder,

$$A_n(x)=A_n(x)^s=-\frac{J_n(x)}{H_n^{(1)}(x)} \tag{3}$$

where p_0 is the incident pressure amplitude, ε_n is the Neumann factor ($\varepsilon_n=2-\delta_{n0}$), J_n and $H_n^{(1)}$ are the Bessel function and the Hankel function of the first kind, respectively. The prime denotes differentiation with respect to the argument. By using the asymptotic form of

Hankel function, the far-field scattered pressure can be expressed as

$$P_{sc}(\phi) = p_0 e^{ikr}\sqrt{\frac{2}{\pi ikr}}\sum_{n=0}^{\infty}\varepsilon_n A_n(x)\cos n\phi, r >> a. \quad (4)$$

The form function f_∞ is defined as an infinite summation of normal modes or partial waves with normal mode number n :

$$f_\infty(\phi) = \sqrt{\frac{r}{a}}\frac{P_{sc}}{p_0}e^{-ikr} = \sum_{n=0}^{\infty} f_n(\phi)$$

$$= \sqrt{\frac{2}{\pi ix}}\sum_{n=0}^{\infty}\varepsilon_n A_n(x)\cos n\phi \quad (5)$$

2. Elastic Wave Scattering

2.1 P wave incidence case

A plane P (Longitudinal) wave incident along the X axis can be expressed as a partial wave series :

$$\varphi_{inc} = \varphi_0 \exp i(k_p X - \omega t),$$

$$= \varphi_0\sum_{n=0}^{\infty}\varepsilon_n i^n J_n(k_p r)\cos n\phi \quad (6)$$

where $k_p = \omega / c_p$ is the longitudinal wave number. In Eq. (6) the time dependence $\exp(-i\omega t)$ is omitted in the right hand side because steady state is being studied. It produces scattered elastic waves which have the following form of potentials :

$$\varphi_{sc} = \sum_{n=0}^{\infty}\varepsilon_n i^n A_n H_n^{(1)}(k_p r)\cos n\phi, \quad (7)$$

and

$$\psi_{sc} = \sum_{n=0}^{\infty}\varepsilon_n i^n B_n H_n^{(1)}(k_s r)\sin n\phi, \quad (8)$$

where $k_s = \omega / c_s$ is the transversal wave number.

Equations (7) and (8) represent outgoing P and S(Shear) waves with wave number k_p and k_s, respectively. In Eq. (8) the incident P wave generates an outgoing S wave, which represents a phenomenon known as mode conversion. By applying a set of appropriate boundary conditions, the unknown scattering coefficients A_n and B_n are determined as[4,6,9] :

For a rigid cylinder,

$$A_n^r = \begin{vmatrix} -\mathrm{Re}\,a_{11} & a_{12} \\ -\mathrm{Re}\,a_{21} & a_{22} \end{vmatrix} \Big/ \begin{vmatrix} a_{11} & a_{12} \\ a_{21} & a_{22} \end{vmatrix}, \quad (9a)$$

$$B_n^r = \begin{vmatrix} a_{11} & -\mathrm{Re}\,a_{12} \\ a_{21} & -\mathrm{Re}\,a_{22} \end{vmatrix} \Big/ \begin{vmatrix} a_{11} & a_{12} \\ a_{21} & a_{22} \end{vmatrix}, \quad (9b)$$

where

$a_{11} = x_p H_n^{(1)\prime}(x_p), a_{12} = nH_n^{(1)}(x_s), a_{21} = -nH_n^{(1)\prime}(x_p),$

$a_{22} = -x_s H_n^{(1)\prime}(x_s)$, $x_{p,s} = k_{p,s}a$ and the superscript r denotes rigid.

For a soft cylinder,

$$A_n^s = \begin{vmatrix} -\mathrm{Re}\,b_{11} & b_{12} \\ -\mathrm{Re}\,b_{21} & b_{22} \end{vmatrix} \Big/ \begin{vmatrix} b_{11} & b_{12} \\ b_{21} & b_{22} \end{vmatrix}, \quad (10a)$$

$$B_n^s = \begin{vmatrix} b_{11} & -\mathrm{Re}\,b_{11} \\ b_{21} & -\mathrm{Re}\,b_{21} \end{vmatrix} \Big/ \begin{vmatrix} b_{11} & b_{12} \\ b_{21} & b_{22} \end{vmatrix}, \quad (10b)$$

where

$b_{11} = -x_s^2 H_n^{(1)}(x_p) - 2x_p H_n^{(1)\prime}(x_p) + 2n^2 H_n^{(1)}(x_p),$

$b_{12} = -2nH_n^{(1)}(x_s) + 2nx_s H_n^{(1)\prime}(x_s),$

$b_{21} = 2nH_n^{(1)}(x_p) - 2nx_p H_n^{(1)\prime}(x_p),$

$b_{22} = x_s^2 H_n^{(1)}(x_s) + 2x_s H_n^{(1)\prime}(x_s) - 2n^2 H_n^{(1)\prime}(x_s),$

and the superscript s denotes soft.

The far field form function f_∞ is defined as an infinite summation of partial waves :

$$f_\infty^{PP}(\phi) = \sum_{n=0}^{\infty} f_n^{PP}(\phi) = \sqrt{\frac{2}{\pi ix_p}}\sum_{n=0}^{\infty}\varepsilon_n A_n \cos n\phi, \quad (11)$$

$$f_\infty^{ps}(\phi) = \sum_{n=0}^{\infty} f_n^{ps}(\phi) = \sqrt{\frac{2}{\pi ix_s}}\sum_{n=0}^{\infty}\varepsilon_n B_n \sin n\phi. \quad (12)$$

2.2 S wave incidence case

A plane S wave incident along the X axis can be expressed as a partial wave series :

$$\psi_{inc} = \psi_0 \exp i(k_s X - \omega t) = \psi_0\sum_{n=0}^{\infty}\varepsilon_n i^n J_n(k_s r)\cos n\phi \quad (13)$$

In Eq. (13) the time dependence $\exp(-i\omega t)$ is omitted in the right hand side because steady

state is being studied. It produces scattered elastic waves which have the following form of potentials:

$$\varphi_{sc} = \sum_{n=0}^{\infty} \varepsilon_n i^n C_n H_n^{(1)}(k_p r)\sin n\phi \quad (14)$$

and

$$\psi_{sc} = \sum_{n=0}^{\infty} \varepsilon_n i^n D_n H_n^{(1)}(k_s r)\cos n\phi \quad (15)$$

By applying a set of boundary conditions, the unknown scattering coefficients C_n and D_n are determined as[4,6,9] :

For a rigid cylinder,

$$C_n^r = \begin{vmatrix} -\mathrm{Re}c_{12} & c_{12} \\ -\mathrm{Re}c_{22} & c_{22} \end{vmatrix} \Big/ \begin{vmatrix} c_{11} & c_{12} \\ c_{21} & c_{22} \end{vmatrix} \quad (16a)$$

$$D_n^r = \begin{vmatrix} c_{11} & -\mathrm{Re}c_{12} \\ c_{21} & -\mathrm{Re}c_{22} \end{vmatrix} \Big/ \begin{vmatrix} c_{11} & c_{12} \\ c_{21} & c_{22} \end{vmatrix}, \quad (16b)$$

where, $c_{11} = a_{11}$, $c_{12} = -a_{12}$, $c_{21} = -a_{21}$, $c_{22} = a_{22}$ and a_{ij} is defined in Eq. (9).

For a soft cylinder,

$$C_n^s = \begin{vmatrix} -\mathrm{Re}d_{12} & d_{12} \\ -\mathrm{Re}d_{22} & d_{22} \end{vmatrix} \Big/ \begin{vmatrix} d_{11} & d_{12} \\ d_{21} & d_{22} \end{vmatrix}, \quad (17a)$$

$$D_n^s = \begin{vmatrix} d_{11} & -\mathrm{Re}d_{12} \\ d_{21} & -\mathrm{Re}d_{22} \end{vmatrix} \Big/ \begin{vmatrix} d_{11} & d_{12} \\ d_{21} & d_{22} \end{vmatrix}, \quad (17b)$$

where, $d_{11} = b_{11}$, $d_{12} = -b_{12}$, $d_{21} = -b_{21}$, $d_{22} = b_{22}$ and b_{ij} is defined in Eq. (10).

The far field form function f_∞ is defined as an infinite summation of partial waves :

$$f_\infty^{sp}(\phi) = \sum_{n=0}^{\infty} f_n^{sp}(\phi) = \sqrt{\frac{2}{\pi i x_p}} \sum_{n=0}^{\infty} \varepsilon_n C_n \sin n\phi \quad (18)$$

$$f_\infty^{ss}(\phi) = \sum_{n=0}^{\infty} f_n^{ss}(\phi) = \sqrt{\frac{2}{\pi i x_s}} \sum_{n=0}^{\infty} \varepsilon_n D_n \cos n\phi \quad (19)$$

3. Numerical Analysis and Discussion

For numerical calculations, the fluid or elastic medium is assumed to be water or aluminum, respectively. The longitudinal wave speed of water is 1480 m/sec, and the longitudinal and transversal wave speeds of aluminum are 6370 and 3070 m/sec, respectively. All numerical calculations are performed for backscattering, that is, $\phi = \pi$.

3.1 Rigid cylinder

Figure 2 compares magnitudes and phases of

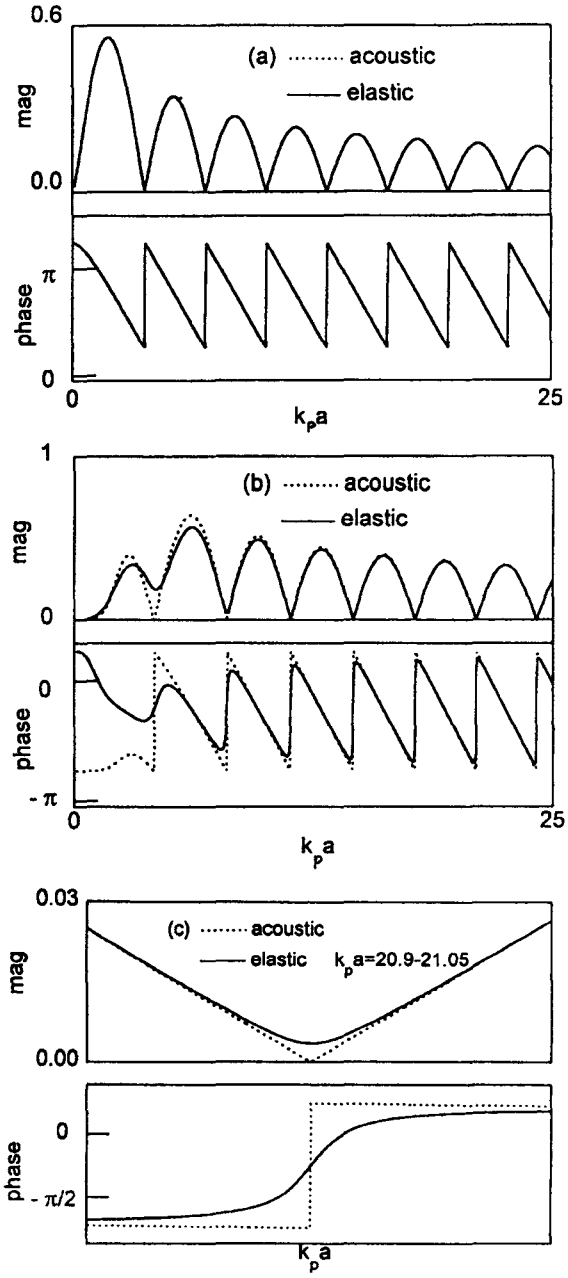

Fig. 2 Acoustic and elastic wave scattering from a rigid cylinder: (a) PP $n=0$ (b) PP $n=3$ (c) PP $n=3$ zoomed plot

partial waves of the elastic rigid PP case (P wave incidence and P wave scattering) with the acoustic rigid case. These two cases are comparable because we have only PP case for the acoustic wave scattering. For $n=0$ mode, mode conversion does not occur for the elastic wave scattering. Therefore, in Fig. 2(a) we obtain identical magnitude and phase for both cases. We note that the dips in the magnitude between two neighboring smooth peaks reaches zero and abrupt π-phase shifts occur at dip frequencies. The amount of phase shifts through the peaks are also π radians. For $n \geq 1$, while acoustic wave scattering retains this behavior, elastic wave scattering does not. As an example, for $n=3$, Fig. 2(b) and (c) show that the magnitudes never reach the zero even at the dips, and the phase shifts at the dips as well as through the smooth peaks are less than π radians. (In References 10 and 11, it is mentioned that this non-zero (filled- in) dip is due to mode conversion and radiation damping. However, we note that radiation damping is not contributing to this filled-in dip because acoustic scattering does not show any filled-in dip.) These phenomena are more apparent in the low frequency region as shown in Fig. 2(b). As the frequency becomes higher, at dip frequencies the magnitudes approach zero value and the phase shifts become close to π. Fig. 2(c) shows clearly that the phase shift at a dip for elastic wave scattering is not abrupt but gradual. These phenomena are due to mode conversion. The energy of incidence P wave is partially converted to that of S wave during elastic wave scattering when $n \geq 1$. By introducing the analogy of mechanical vibration system, PP case acts like a system with damped oscillators, in which the phase shift at a resonance is gradual and less than π due to the energy dissipation by damping and the overlapping of neighboring resonances. The amount of mode converted energy is larger in the low frequency region and becomes smaller as the frequency increases, as shown in PS case (P wave incidence and S wave scattering) in Fig. 3. The elastic PS case looks much simpler than PP

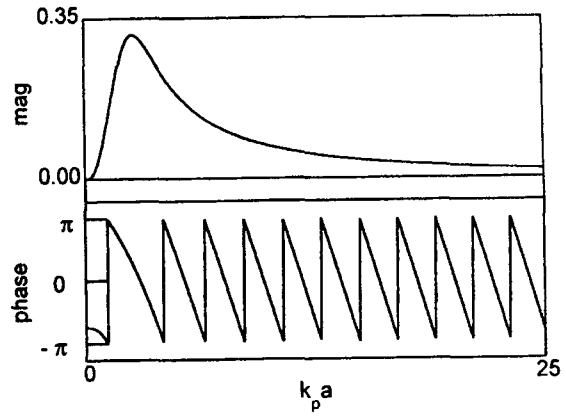

Fig. 3 Elastic wave scattering from a rigid cylinder : PS $n=3$

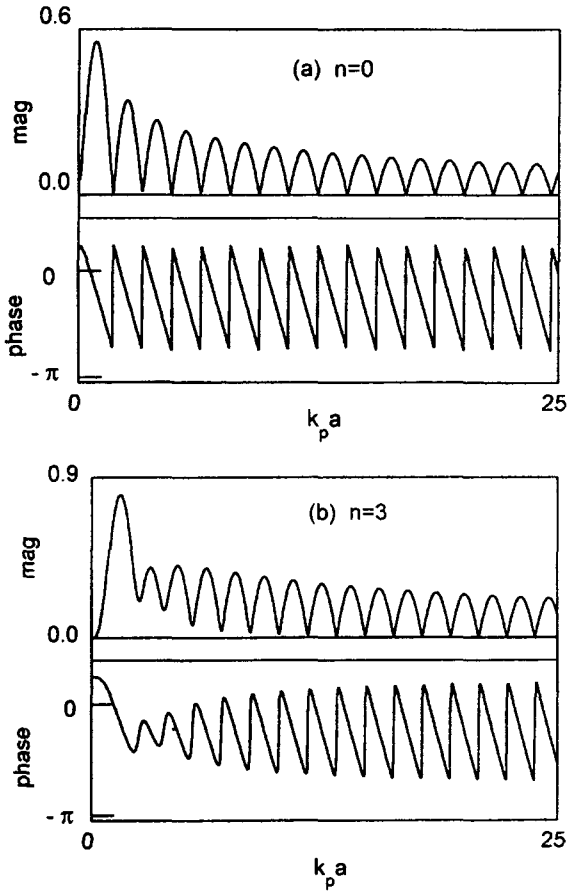

Fig. 4 Elastic wave scattering from a rigid cylinder : (a) SS $n=0$ and (b) SS $n=3$

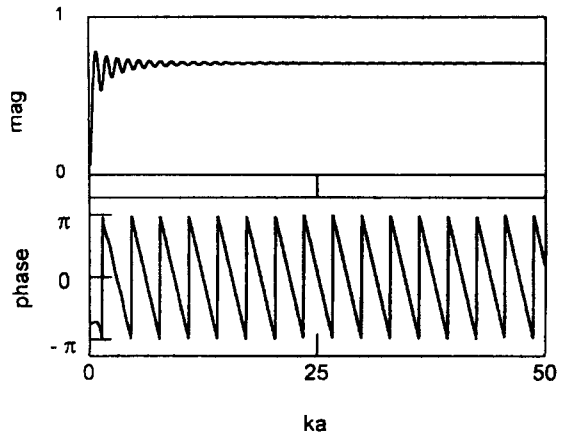

Fig. 5 Form function of acoustic wave scattering from a rigid cylinder

case. There is only one smooth peak in the magnitude which moves to the right as the mode number n increases, and therefore no dip exists. The phase goes down monotonously without any abrupt shift as the frequency increases. Due to the unitarity of the scattering matrix[4,6], the PS and *SP* cases are identical (except the different level of magnitude). Figure 4 presents the *SS* case. Similarly to the *P* wave incidence case, there is no mode conversion when $n = 0$. Figure 4(a) shows that for $n = 0$ mode, dips reach zero in magnitude and π-phase shifts take place at the dip frequencies and also through smooth peaks. (We note that if Fig. 4(a) is plotted as a function of ka rather than $k_p a$, it would be the identical plot with Fig. 2(a).) Like the *PP* case, for $n \geq 1$, the dips do not reach down to zero value and the phase shifts are less than π radians because of mode conversion, as shown in Fig. 4(b).

The form functions are obtained by summing partial waves as defined. Figs. 5 and 6 show the form functions of the acoustic and elastic wave scatterings, respectively. The magnitudes of the form functions for non-mode conversion cases (*PP* or *SS*) converges to the same value of $1/\sqrt{2}$ for both acoustic and elastic wave

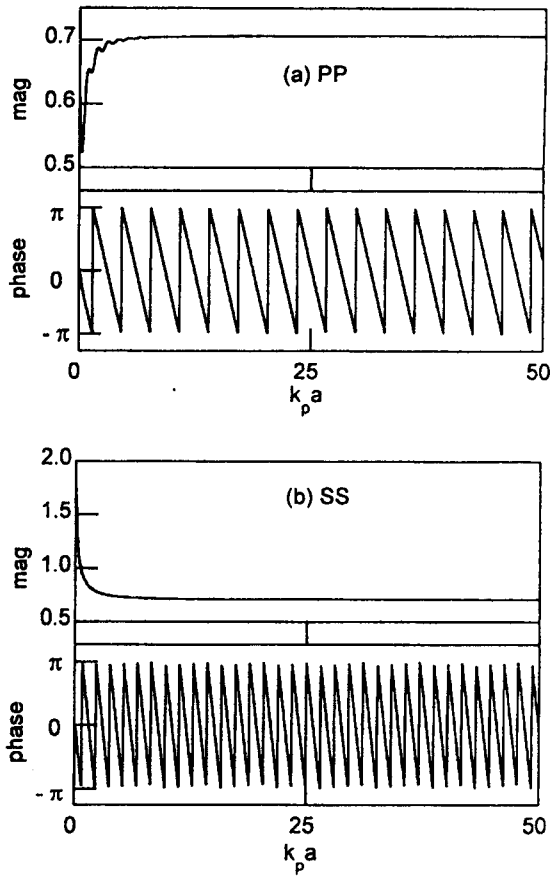

Fig. 6 Form function of elastic wave scattering from a rigid cylinder : (a) *PP* and (b) *SS*

scatterings. The phases are monotonously decreasing without any abrupt or gradual phase shift throughout all frequency range although each partial wave includes phase shifts at the dip frequencies.

3.2 Soft cylinder

Basically the same trends in the behaviors of magnitudes and phases can be observed for both the rigid and soft cylinder cases. Therefore, the detailed discussion is not repeated for the soft cylinder case.

Elastic soft *PP* $n = 0$ mode in Fig. 7(a) behaves differently from acoustic soft $n = 0$ mode, especially, near zero frequency, while we had identical plots for elastic rigid *PP* and acoustic rigid for $n = 0$ mode (Fig. 2(a)). Figure 7(b) shows the effect of mode conversion on the

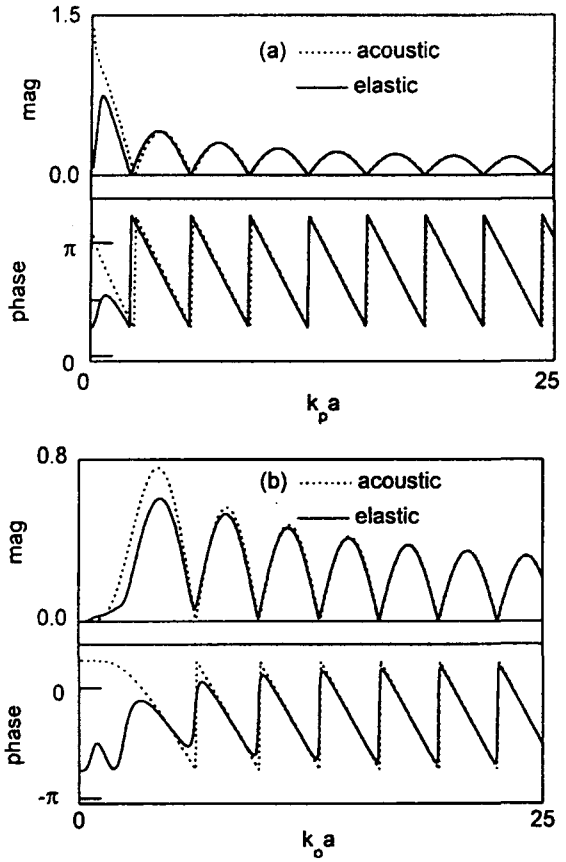

Fig. 7 Acoustic and elastic wave scattering (*PP*) from a soft cylinder: (a) $n=0$ and (b) $n=3$

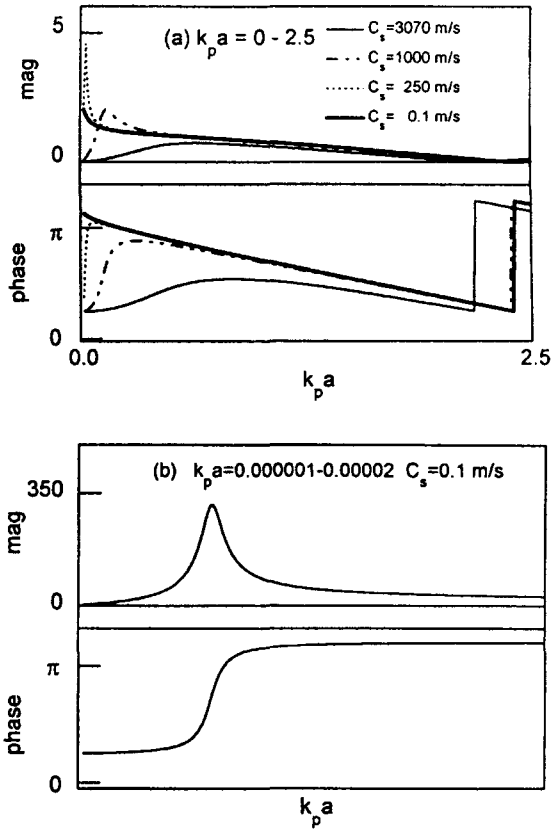

Fig. 8 Elastic wave scattering (*PP*) from a soft cylinder with a varying c_s : (a) $n=0$, $k_p a = 0$ - 2.5 and (b) $n=0$, $k_p a$ = 0.000001 - 0.00002

magnitude and phase, similarly to Fig. 2(b). A parametric study was performed in Fig. 8, where the shear wave velocity c_s of the elastic medium is arbitrarily decreased from 3070 m/s to 0.1 m/s to simulate acoustic wave scattering. As c_s decreases, a larger peak is clearly shown of which location is moving to the zero frequency. For $c_s=0.1$ m/s, it shows almost same magnitude and phase with the acoustic $n=0$ mode (Fig. 8(a)). However, more detailed calculation reveals that there is still a very large peak near zero frequency as can be seen in Fig. 8(b). This peak was mentioned as a giant monopole elsewhere[10]. Therefore, we can see that the giant monopole is caused by diminishing shear wave velocity c_s due to the loss of shear resistance in the medium. *PS* case shown in Fig. 9 presents two smooth peaks (of which locations are moving to the high frequency region and of which magnitudes decrease as the mode number increases). The phase monotonously goes down through the second peak. A dip existing between these two peaks reaches zero in magnitude and the abrupt phase shift of π occurs at the dip frequency. This dip moves to the right as the mode number n increases[4]. This behavior of elastic soft *PS* case looks different from *PP* case ($n \geq 1$) and can be explained as such: There is an energy loss in *PP* case, and consequently *PS* case earns the energy which *PP* loses. Therefore, elastic soft *PS* case is not comparable to a damped oscillator, but rather a negatively damped one. Figure 9 also shows that the dip exists at the exactly same frequency for

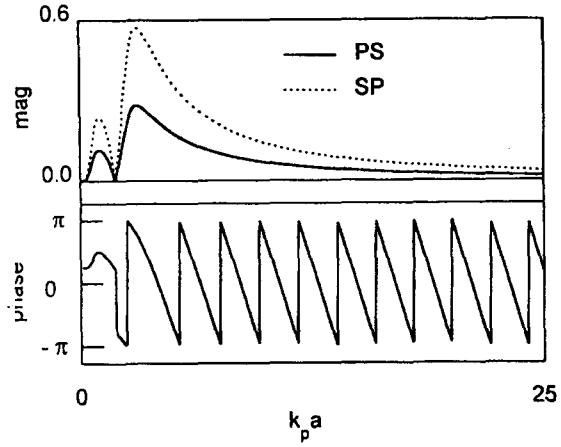

Fig. 9 Elastic wave scattering (*PS* and *SP*) from a soft cylinder for $n=3$

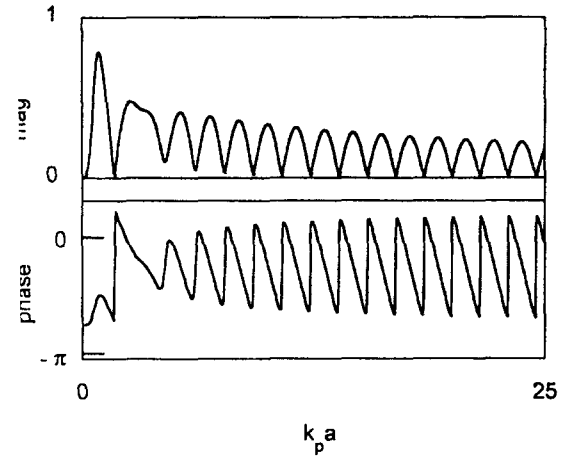

Fig. 10 Elastic wave scattering (*SS*) from a soft cylinder for $n=3$

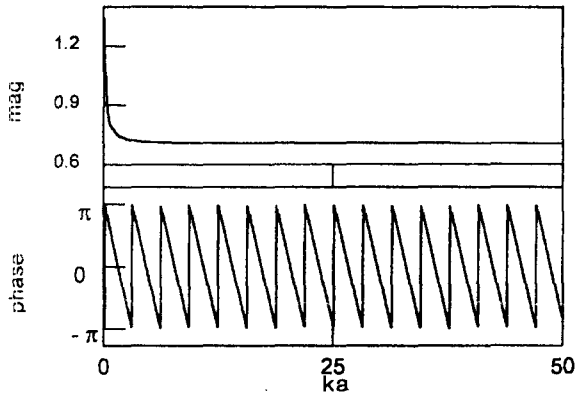

Fig. 11 Form function for acoustic wave scattering from a soft cylinder

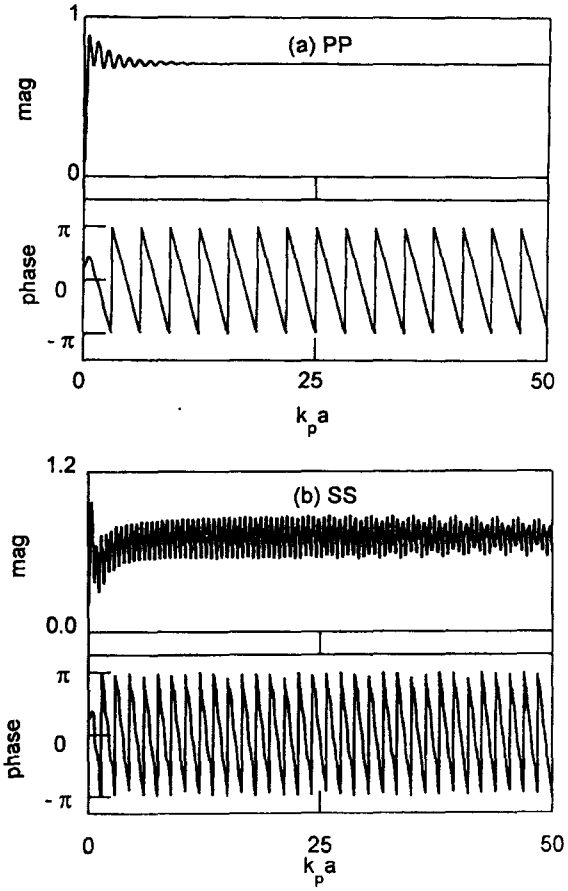

Fig. 12 Form function for elastic wave scattering from a soft cylinder : (a) *PP* and (b) *SS*

both PS and SP cases. As shown in Fig. 10, we observe that for SS cases when $n \geq 2$, the first dip from the left side is very close to zero magnitude and the phase shift is close to π radians at that frequency. This is because the mode converted energy is very small near this first dip frequency as can be seen in Fig. 9.

The form functions can be obtained by summing partial waves. Figs. 11 and 12 show the form functions of acoustic and elastic wave scatterings, respectively. It is interesting to observe that the acoustic soft (Fig. 11) and elastic soft *PP* (Fig. 12(a)) cases look similar to the elastic rigid *SS* (Fig. 6(b)) and acoustic rigid (Fig. 5) cases, respectively. The form function for elastic soft *SS* case in Fig. 12(b) appears to be the most noteworthy shape. It is due to the characteristics of interference

between two shear waves from the reflection from and diffraction around the soft cylinder.

4. Conclusions

Acoustic and elastic wave scatterings from an acoustically rigid or soft cylinder were numerically analyzed, and the characteristics of phase and magnitude of the scattered waves were studied. The effect of mode conversion, which occurs during elastic wave scattering, on the magnitude and phase of partial waves of scattered waves is identified. In case of non-mode conversion in the acoustic or elastic wave scattering, the dip between smooth peaks in each partial wave reaches the zero magnitude and abrupt π-phase shift occurs at the dip frequency. However, for mode conversion cases, the dip never reaches zero magnitude, and the phase shift becomes gradual and less than π radians. The phase of the form functions do not show any abrupt phase change throughout all frequency ranges for both acoustic and elastic wave scatterings.

References

(1) Strutt, J. W. (Rayleigh), 1896, The Theory of Sound, 2nd Ed., Vol. II, Macmillan.

(2) Morse, P. M. and Ingard, K. U., 1968, Theoretical Acoustics, McGraw-Hill.

(3) Bowman, J. J., Senior, T. B. A. and Uslenghi, O. L. E, 1969, Electromagnetic and Acoustic Scattering by Simple Shapes, Wiley.

(4) Rhee, Huinam and Park, Youngjin, 1997, "Novel Acoustic Wave Resonance Scattering Formalism", J. Acoust. Soc. Am., 102(6), pp. 3401~3412.

(5) Flax, L., Dragonette, L. R., and Uberall, H., 1978, "Theory of Elastic Resonance Excitation by Sound Scattering", J. Acoust. Soc. Am. 63(3), pp. 723~731.

(6) Flax, L., Gaunaurd, G., and Uberall, H., 1981, "Theory of Resonance Scattering", in Physical Acoustics, Edited by Mason, W. P., and Thurston, R. N., Vol.XV, pp. 191~294, Acamedic, New York,

(7) Veksler, N. D., 1993, "Resonance Acoustic Spectroscopy", Springer-Verlag.

(8) Rhee, Huinam, 1998, "Novel Formalism for Resonance Scattering of Acoustic and Elastic Waves", Ph. D thesis, KAIST.

(9) Rhee, Huinam and Youngjin Park, 1997, "Acoustic and Eastic Wave Scattering from a Rigid or Soft Cylinder", Proceedings of the 5th Int. Congress on Sound and Vibration, Univ. of Adelaide, Australia.

(10) Gaunaurd, G. C. and Uberall, H., 1978, "Theory of Resonance Scattering from Spherical Cavities in Elastic and Viscoelastic Media", J. Acous. Soc. Am., 63(6), pp. 1699~1712.

(11) Gaunaurd, G. C. and Uberall, H., 1979, "Numerical Evaluation of Modal Resonances in the Echoes of Compressional Waves Scattered from Fluid-filled Spherical Cavities in Solids", J. Appl. Phys. 50(7), pp. 4642~4660.